Monatshefte für Chemie 136, 1947–1953 (2005)
DOI 10.1007/s00706-005-0396-6

Monatshefte für Chemie
Chemical Monthly
Printed in Austria

Primary Transformation Rate Measurements Through Differential Scanning Calorimetry

Maria-Teresa Clavaguera-Mora[1,*], **Narcís Clavaguera**[2], and **Javier Rodríguez-Viejo**[1]

[1] Grup de Física de Materials I, Departament de Física, Universitat Autònoma de Barcelona, 08193-Bellaterra, Spain
[2] Grup de Física de l'Estat Sòlid, Departament ECM, Facultat de Física, Universitat de Barcelona, 08028-Barcelona, Spain

Received September 12, 2004; accepted February 2, 2005
Published online November 14, 2005

Summary. The primary crystallization of molten alloy systems at high undercooling is studied by a precise quantitative analysis of the calorimetric signal obtained during the transformation in terms of the reaction rate under isothermal and continuous heating regimes. It is shown that, under specific conditions, namely, stoechiometric primary precipitates, generalized relationships for the crystallization enthalpy and the reaction rate may be obtained.

Keywords. DSC; Reaction kinetics; Alloys; Crystallization.

Introduction

Suitable transformations for this study are first order reactions, accompanied by energy exchanges with the environment, which allow thermal or calorimetric measurements. Several transformation characteristics, such as the onset temperatures of phase changes, enthalpy of transformation, and the evolution of the transformed volume fraction, ξ, are currently obtained. Nowadays, the quantitative analysis of the kinetics of the transformation becomes vital in many instances for process optimization. The quantitative kinetic analysis is grounded on data on the reaction rate, which in a calorimetric experiment is assumed proportional to the heat flow generated by the transformation. Both differential thermal analysis (DTA) and differential scanning calorimetry (DSC) are currently used to determine kinetic data on transformations.

Information on the mechanisms driving the transformation relies on analysis of the precise form of the calorimetric signal. For instance, it has been proven that the shape characteristics of the isothermal calorimetric signal can identify

* Corresponding author. E-mail: mtmora@vega.uab.es

unambiguously grain growth in microcrystalline materials *versus* nucleation and growth of amorphous powders [1, 2]. More recently, the shape of the DSC primary crystallization peaks of amorphous metallic alloys, in particular, the high-temperature tails observed under non-isothermal regime, have been related to the crystallite coarsening [3]. In primary crystallization from an undercooled molten alloy it is very important to get experimental information on the diffusion limiting effects. Then, the analysis of the heat flow evolution and particle growth rate, including soft impingement and multicomponent diffusion paths become of prime interest [4–6]. The utility of DSC for investigating the thermodynamics and kinetics of a broad range of thin films' reactions has also been demonstrated [7].

Several hypotheses, often implicit, are needed to get the relationship between calorimetric data and kinetic parameters. This paper deals with a revision of either implicit or explicit assumptions used to get the time evolution of the degree of advancement of a thermally activated transformation. In particular, in a recent paper, it is claimed that there is a non-linear relationship between the evolved enthalpy, obtained from DSC experiments, and the transformed fraction during primary crystallization [8].

Non-equilibrium Primary Crystallization

In DSC data analysis, the kinetic data are obtained from the DSC signal evolution with time/temperature. The primary data is the heat flux (height of the DSC curve) during the transformation, which is obtained by subtracting the base line (DSC signal without transformation) from the DSC signal. The volume fraction of material transformed ξ at a given time t (or temperature T) is determined from the ratio between the subtended area of the DSC peak at that time (temperature) and the area of the complete exothermic (or endothermic) transformation peak. Similarly, the transformation rate $\dot{\xi}$ is determined as the ratio between the height of the DSC curve at that time or temperature and the complete area. That is, the rate of heat generated during the transformation process is proportional to the transformation rate (Eq. (1)) where ΔH is the transformation enthalpy.

$$\dot{\xi} = \frac{1}{\Delta H}\frac{dQ}{dt} \tag{1}$$

This statement is assumed to be true for eutectic- and polymorphous-type transformations; however, it is recognized that it becomes, at most, a first approximation for a primary crystallization process [5, 8]. Our purpose is to discuss in detail the dependence of the rate of enthalpy generated, dH/dt, on the crystallization rate $\dot{\xi}$ when both the crystalline nuclei and the disordered matrix compositions are different and may change during the process. The following discussion is focused in primary crystallization processes from a disordered or undercooled liquid state.

Let us consider the values of the specific enthalpy, H_t, at any intermediate stage of the process, where the subscript t indicates its time dependence through any of the variables T or ξ. At time t, the primary transformation has evolved up to a fraction, $\xi \cdot f_1$, of the total volume, V, where f_1 is the total volume fraction available for primary crystallisation. In terms of enthalpy, a volume fraction $\xi \cdot f_1$ is in crystalline form and has a specific enthalpy $H_t^{xt}(c_1^{xt}, \ldots, c_{n-1}^{xt}, T, p)$ whereas a

volume fraction $(1-\xi\cdot f_1)$ remains in disordered state and has a specific enthalpy $H_t^{\ell}(c_1^{\ell},\ldots,c_{n-1}^{\ell},T,p)$, where p stands for pressure and c_i^{xt} and c_i^{ℓ} are the concentrations of each component i $(i=1,\ldots,n)$ in the crystalline phase and in the undercooled liquid, respectively. Furthermore, assuming a stoechiometric crystalline phase, the concentrations, c_i^{ℓ} change along the transformation in the form shown by Eqs. (2) and (3) [7] where $c_i^{\ell,o}=c_i^{\ell}(\xi=0)$ and $c_i^{\ell,*}=c_i^{\ell}(\xi=1)$, respectively, are the concentration of component i in the initial undercooled liquid and in the liquid in stable/metastable equilibrium with the primary crystals.

$$c_i^{\ell}(f_1\cdot\xi,T)=\frac{c_i^{\ell,o}-f_1\cdot\xi\cdot c_i^{xt}}{1-f_1\cdot\xi} \tag{2}$$

$$f_1=\frac{c_i^{\ell,*}-c_i^{\ell,o}}{c_i^{\ell,*}-c_i^{xt}} \tag{3}$$

Taking in account that the specific enthalpy of the stable/metastable mixture of primary crystals and disordered phase is given by Eq. (4) the heat evolved from the sample changes at a rate (see Appendix) shown by Eq. (5) with h_i^{xt}, h_i^{ℓ} the partial molar enthalpy of component i in each phase, β the scan rate, and $f_1\cdot\Delta C_p$ given by Eq. (6) provided the partial specific heat of the liquid components is quite insensitive to compositional changes, $C_{p,i}^{\ell}\approx C_{p,i}^{\ell,o}\approx C_{p,i}^{\ell,*}$, and assuming there is a negligible change of f_1 with temperature. Also, the crystallization enthalpy is given by Eq. (7).

$$H_t^{*}=f_1\cdot H_t^{xt}+(1-f_1)H_t^{\ell,*} \tag{4}$$

$$\begin{aligned}\frac{dQ}{dt}&=-\frac{d}{dt}[f_1\cdot\xi\cdot H_t^{xt}+(1-f_1\cdot\xi)H_t^{\ell}-H_t^{*}]\\&=f_1\cdot\dot{\xi}\sum_i c_i^{xt}(h_i^{\ell}-h_i^{xt})-\beta\cdot f_1\cdot(1-\xi)\cdot\Delta C_p\end{aligned} \tag{5}$$

$$\begin{aligned}f_1\cdot\Delta C_p&=C_p^{\ell,o}-f_1C_p^{xt}-(1-f_1)C_p^{\ell,*}\\&=f_1\sum_i c_i^{xt}(C_{p,i}^{\ell,*}-C_{p,i}^{xt})\end{aligned} \tag{6}$$

$$\Delta H_{xt}=H^{\ell,o}-f_1H^{xt}-(1-f_1)H^{\ell,*} \tag{7}$$

Isothermal Regime

Under isothermal regime, the normalised height of the DSC curve becomes as shown by Eqs. (8) and (9).

$$\frac{1}{\Delta H_{xt}}\frac{dQ}{dt}^{\mathrm{ISO}}=\dot{\xi}\cdot F(f_1\cdot\xi) \tag{8}$$

$$F(f_1\cdot\xi)=\frac{f_1\sum_i c_i^{xt}(h_i^{\ell}-h_i^{xt})}{\Delta H_{xt}} \tag{9}$$

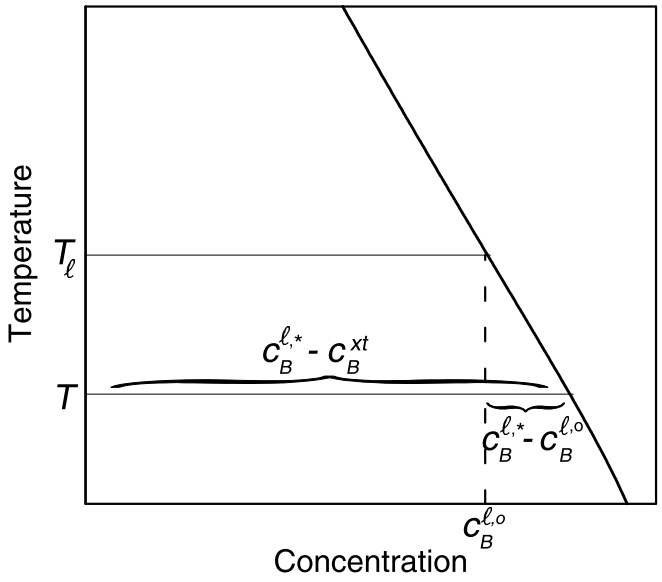

Fig. 1. Rich A region of the stable/metastable A–B phase diagram for a binary regular liquid solution and no miscibility of component B in solid A

If $h_i^{\ell,o} = h_i^{\ell} = h_i^{\ell,*}$, irrespective of the composition of the liquid, which would be the case, for instance, for an ideal liquid solution, then Eq. (1) is satisfied. In general $h_i^{\ell,o} \neq h_i^{\ell} \neq h_i^{\ell,*}$, therefore, let us consider, as an example, the primary crystallisation of crystalline A in a binary undercooled regular liquid solution of overall composition $c_B^{\ell,o}$. Its stable/metastable phase diagram, depicted in Fig. 1, corresponds to the situation where the interaction energy, Ω, between components A and B is negative or, equivalently, for a deep eutectic system as is normally the case for glass forming alloy compositions. That is, the change of the partial molar enthalpy of each component in the liquid phase at constant temperature and pressure occurs as a consequence of the continuous compositional change of the liquid during the reaction, as shown by Eq. (10) with Δh_f^i being the melting enthalpy of component i, and x_i the molar fraction of component i ($x_i = V_m \cdot c_i$, with V_m the molar volume).

$$h_i^{\ell}(c_B^{\ell}) = \Delta h_f^i + h_i^{xt} + \Omega(1 - x_i^{\ell})^2 \tag{10}$$

The time evolution of $F(f_1 \cdot \xi)$ has been computed for different situations. In Fig. 2 it is plotted as a function of ξ for a fixed annealing temperature and different degrees of supersaturation (varying $x_B^{\ell,o}$). It is observed that $F(f_1 \cdot \xi)$ is close to 1, but its value is lager than one at the onset of the transformation, and it becomes lower than one at the last steps of the transformation, the lowest value being obtained for large supersaturation values.

Another possible situation is depicted in Fig. 3. It represents the time evolution of $F(f_1 \cdot \xi)$ for an overall fixed composition $x_B^{\ell,o}$, and different annealing

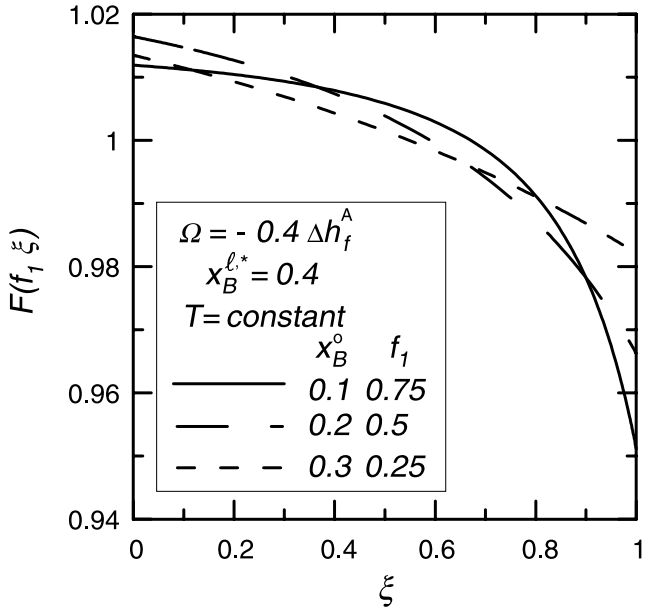

Fig. 2. Plot of the evolution of $F(f_1 \cdot \xi)$ as a function of ξ at a fixed temperature, for three different alloy compositions

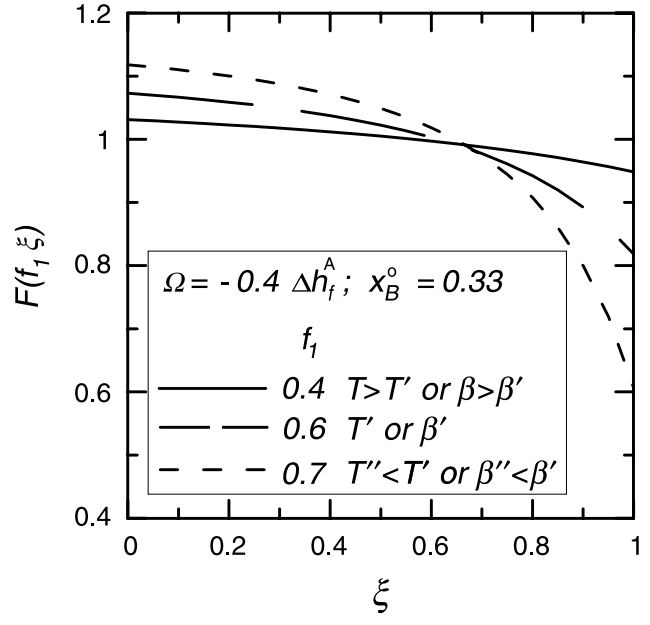

Fig. 3. Plot of the evolution of $F(f_1 \cdot \xi)$ as a function of ξ for an overall composition $x_B^{\ell,o}$, at different annealing temperatures

temperatures. Again, the largest is the degree of supersaturation the lowest becomes $F(f_1 \cdot \xi)$ (or ratio between the normalised height of the DSC curve and the reaction rate) at the last steps of the transformation.

Continuous Heating Regime

Under continuous heating regime, the normalised height of the DSC curve becomes as shown by Eq. (11).

$$\frac{1}{\Delta H_{xt}}\frac{dQ^{C.H.}}{dt} = \dot{\xi}\cdot F(f_1\cdot\xi) - \frac{f_1(1-\xi)\beta}{\Delta H_{xt}}\Delta C_p \qquad (11)$$

It is generally recognised that a very useful concept is the ''hypothetical'' signal that will represent the enthalpy changes not directly related to the reaction rate (mostly due to specific heat capacity changes of the initial or product phases) [5]. This hypothetical signal is most often called *base line shift*. This effect is clearly indicated in Eq. (11) whose second right hand term represents the influence of the change on heat capacity in the calorimetric signal.

With respect to the first right hand term of Eq. (11), experimentally the temperature range in which the transformation proceeds under continuous heating is normally quite narrow. Consequently, neglecting the heat capacity contribution in the calorimetric signal, the preceding analysis may be easily extended to continuous heating since to increase the heating rate is equivalent to shift the transformation onset towards higher temperatures. Such an extension is schematically presented in Fig. 3. As already shown on isothermal regime, the normalised height of the DSC curve is larger than the reaction rate at the initial stages of the transformation. That is, identifying the normalised height of the DSC curve with the *apparent* reaction rate, the transformation starts with a larger than real *apparent* acceleration. However, this effect is not significant when compared with the effect obtained at the latest stages of the transformation. There, the *apparent* deceleration of the reaction is larger than the real one.

Conclusions

The primary crystallization of molten alloy systems at high undercooling has been analyzed by differential scanning calorimetric measurement of the transformation rate. Emphasis is given to the conversion of the evolution of the measured calorimetric signal to reaction rate. The current assumption that the heat flow generated during the transformation is proportional to the reaction rate is shown to be very fruitful. Under specific conditions, namely, stoechiometric primary precipitates and homogeneous remaining liquid composition, generalized relationships for the crystallization enthalpy and the reaction rate from the measured calorimetric signal have been deduced for both, isothermal and continuous heating regimes. It has been demonstrated that, in both regimes, a general prediction for glass forming alloys is that the transformation starts with a larger than real *apparent* acceleration but the *apparent* deceleration of the reaction is larger than the real one.

Acknowledgements

Financial support form ''Generalitat de Catalunya'', through project 2001SGR-00190 and from ''Ministerio de Educación y Ciencia'', through projects MAT2001-2532 and MAT2003-8271 is acknowledged.

Appendix

The specific enthalpy difference between the stable/metastable mixture of primary crystals, with volume fraction f_1; and disordered phase, with volume fraction $(1-f_1)$; and the instantaneous mixture of crystals, with volume fraction $\xi \cdot f_1$; and a disordered phase, with volume fraction $(1-\xi \cdot f_1)$; is given by Eq. (A-1).

$$\begin{aligned} H_t^* - H_t &= f_1 \cdot H_t^{xt} + (1-f_1)H_t^{\ell,*} - f_1 \cdot \xi \cdot H_t^{xt} - (1-f_1 \cdot \xi)H_t^{\ell} \\ &= f_1 \sum_i c_i^{xt} h_i^{xt} + \sum_i (1-f_1) c_i^{\ell,*} h_i^{\ell,*} - f_1 \cdot \xi \sum_i c_i^{xt} h_i^{xt} - \sum_i (1-f_1 \cdot \xi) c_i^{\ell} h_i^{\ell} \end{aligned} \tag{A-1}$$

Assuming there is a negligible change of f_1 with temperature, the rate of change of the several quantities entering in Eq. (A-1) is given by Eqs. (A-2) and (A-3) since $\sum_i c_i^{\ell} dh_i^{\ell}|_{T,p} = 0$ and using the mass balance Eq. (2).

$$\frac{dH_t^{\varphi}}{dt} = \beta C_p^{\varphi} = \beta \sum_i c_i^{\varphi} C_{p,i}^{\varphi} \quad \text{for } \varphi = xt, \ell, * \tag{A-2}$$

$$\frac{d}{dt}(1-f_1 \cdot \xi) \sum_i c_i^{\ell} h_i^{\ell} = (1-f_1 \cdot \xi)\beta \sum_i c_i^{\ell} C_{p,i}^{\ell} + \sum_i h_i^{\ell} \frac{d}{dt}[c_i^{\ell,o} - f_1 \cdot \xi c_i^{xt}] \tag{A-3}$$

Consequently Eq. (A-4) is obtained.

$$\frac{d(H_t^* - H_t)}{dt} = f_1 \cdot \dot{\xi} \sum_i c_i^{xt}(h_i^{\ell} - h_i^{xt}) + \beta[f_1 \cdot \xi(C_p^{\ell} - C_p^{xt}) + (C_p^{\ell,*} - C_p^{\ell}) + f_1(C_p^{xt} - C_p^{\ell,*})] \tag{A-4}$$

If $C_{p,i}^{\ell} \approx C_{p,i}^{\ell,o} \approx C_{p,i}^{\ell,*}$, one obtains Eq. (5).

References

[1] Chen LC, Spaepen F (1988) Nature **336**: 366
[2] Chen LC, Spaepen F (1992) Nano Struct Mater **1**: 59
[3] Jiang XY, Zhong ZC, Greer AL (1997) Mater Sci Eng **A226–228**: 789
[4] Allen DR, Foley JC, Perepezko JH (1998) Acta Mater **46**: 431
[5] Clavaguera N, Clavaguera-Mora MT, Fontana M (1998) J Mater Res **13**: 744
[6] Michaelsen C, Barmak K, Weihs TP (1997) J Phys D Appl Phys **30**: 3167
[7] Clavaguera-Mora MT, Clavaguera N, Crespo D, Pradell T (2002) Prog Mater Sci **47**: 559
[8] Barandiaran JM, Telleria I, Garitaonandia JS, Davies HA (2003) J Non-Cryst Solids **329**: 57